

## Numerical Simulation of Spinning Forming Process of Major Flywheel on DMFW based on Deform

Qiong-Ye LU<sup>1,a\*</sup>, Jun YAN<sup>2</sup>, Fang QU<sup>2</sup>

<sup>1</sup>Automobile and Transportation,Nantong Vocational University,Nantong 226001,China;

<sup>2</sup>Nantong Fuleda Auto Parts Co., LTD, Nantong 226001, China

<sup>a</sup>69865190@qq.com

\*Corresponding author

**Keywords:** DEFORM DMF, spin-forming, numerical simulation

**Abstract.** A mechanical model for major flywheel on DMFW spinning is established by means of the method of elastic-plastic theory, and the forming process of flywheel is simulated numerically with the software Deform-3D. The curves of forming by different revolving feed ratio are presented and the distribution regularity of stress and strain in the forming zone is analyzed. The results are useful to the study of the flywheel spinning and optimization of the technological parameters.

### Introduction

Spin technology is a kind of advanced plastic forming process during which the metal plate blank or preformed blank is struck on the mandrel of spinning machine tightly and continuous plastic deformation is produced point by point depending on the mandrel and forming cutter through mandrel and blank revolving around the shaft, as a result that various shapes of hollow revolution parts can be obtained<sup>[1-5]</sup>. The principle of spinning is in figure 1.

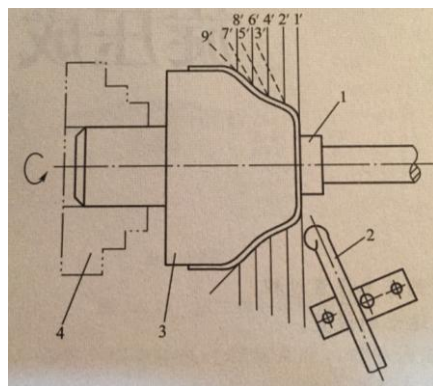


**Fig.1.** Principle of Spinning

1—top block 2—stick 3—mould 4—chunk 1'~9' (location of the continuous billet)

Series of Deform software is developed by science technology co., LTD located in Ohio Columbus in the United States. The deformation and heat transfer characteristics of the object under the action of coupling during the process of metal forming can be analyzed by Deform-3D[6], furthermore stress, strain and temperature distribution considered of deformation heat effect under the heat exchange between the work piece and mould with surrounding medium. The results are useful to optimize metal spinning technology and guide mould design and afford support to manufacture in theory.

Dual Mass Flywheel, simply called DMFW, is divided into two parts by a torsion damper. One is located on the engine side as the role of original flywheel used to start and transfer the rotation torque from engine, called primary weight. The other is located on the side of transmission used to enhance the rotation torque of transmission called secondary weight. There is a ring shape of oil chamber equipped with spring shock absorber between the two flywheel. The spring shock absorber

connects two parts of flywheel into the whole. The structure of DMFW is shown as the figure 2. In a word, dual mass flywheel is the best effective vibration and isolation on the modern automobile[7].

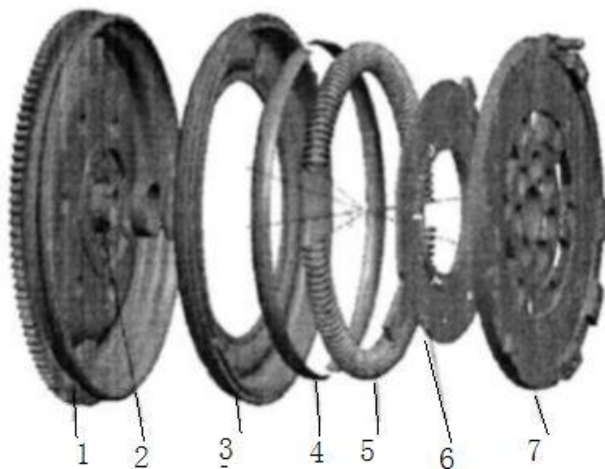


**Fig. 2. Structure of DMFW**

1—ring gear and the main flywheel body 2—flange 3—over plate and the connection ring  
4—slide way 5—arc spring 6—wave-form seal ring 7—deputy flywheel

The traditional method of flywheel is that the cast blank is machined into shape. However, this method is with the disadvantages of complex processing and high cost manufacturing. In this work, the spin forming of flywheel is simulated by soft Deform-3D. The part drawing of flywheel is shown in figure 3. The appropriate process parameters can be discussed and determined to offer the evidence to the feasibility of using the spinning technology according to the distribution regularities analyzed by numerical simulation.

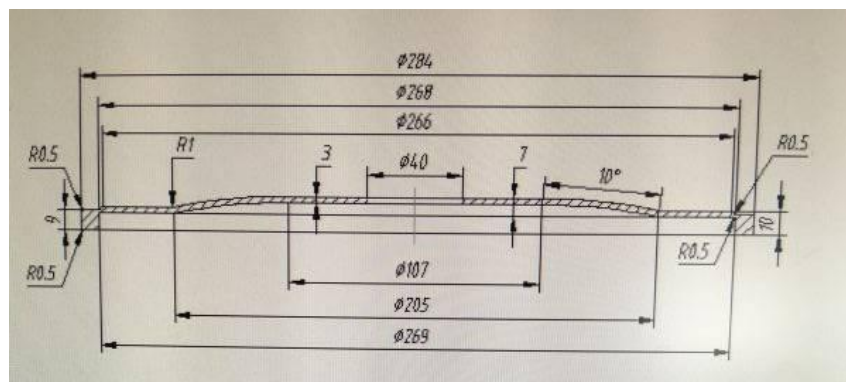


**Fig. 3. Part drawing for some main flywheel**

### Method of Model Establishment

**Establishment of Elastic-plastic Finite Element Model.** The elastic-plastic matrix equation is determined according to the basic theory of finite element of Mises yield criterion in this work and the formula is as follows<sup>[8]</sup>:

$$\Delta\sigma_{ij} = D_{ijkl}\Delta\varepsilon_{ij} \quad (1)$$

where  $\Delta\sigma_{ij}$  is stress increment tensor and  $\Delta\varepsilon_{ij}$  is strain increment tensor and  $D_{ijkl}$  is elastic-plastic matrix . So the formula of  $D_{ijkl}$  is as follows:

$$D_{ijkl} = \frac{E}{1+\mu} [\sigma_{ik}\sigma_{jl} + \frac{\mu}{1+\mu}\sigma_{ij}\sigma_{kl} - \frac{3\sigma^i\sigma^j\sigma^k\sigma^l}{1+\frac{2}{3}H\frac{1+\mu}{E}}] \quad (2)$$

where H is hardening coefficient, E is elasticity modulus,  $\mu$  is poisson ratio and  $\sigma^i$  is stress partial tensor.

The model is established through 3D software PRO/E shown in the figure 4. Then the model is guided into DEFORM-3D in which the model blank is meshed into the number of 5000 tetrahedral mesh by 4-node quadrilateral element, the mesh drawing is in figure 5. Where the blank is defined as elastic plastic body, mandrel and spinning roller are defined as rigid body. It is not needed that the rigid body is defined and meshed.

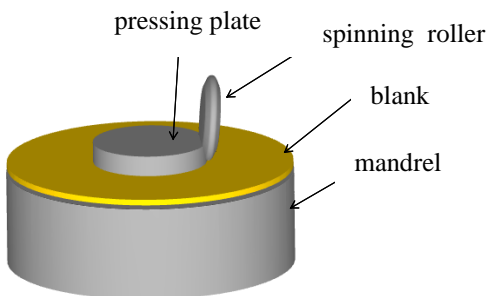


**Fig. 4** Three-dimensional Geometric Model

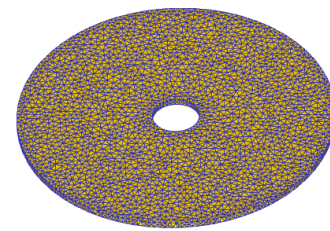


**Fig.5** Meshing figure

**Scheme of Simulation.** The relative movements among the spinning roller, blank and mandrel are more implicated in practical process. On one hand, blank and mandrel are driven by the axis of rotation; On the other hand, the spinning roller is in the motion along the axial feed and rotates around its own axis against its role of friction. When the FEM is established, the mode of relative motion is adopted for the accuracy of simulation and results in the process of spinning. It is supposed that the blank, mandrel and the tail piece are fixed, but the spinning roller is driven by the motion of rotation and axial movement around the X axis (the center axis of rotation) among the blank surface. The friction model based on the shearing strength is simplified after being simulated. The formula of the model is as follows:

$$\sigma_{fr} \leq -m \frac{\bar{\sigma}}{\sqrt{3}} t \quad (3)$$

where m is friction factor,  $\bar{\sigma}$  is resistance to deformation and t is unit vector in the direction of the tangent relative to the direction of sliding velocity. The friction coefficient between the blank and the spinning roller is set to 0.12. The contact point between the blank and mandrel is set into a restrained state. The state between the blank and mandrel is similar to the previous. The displacement of mandrel and top block at the direction of X, Y and Z and the rotational velocity around the three axes are both set to 0. In this case, the simulation spinning process is equivalent to the practical one.

There are a great many of process parameters related to spinning forming of metal materials, such as motion trail of spinning roller, wall thickness reduction, feeding rate of spinning roller, spindle speed and spinning temperature. The room temperature is set to 20 °C considering to be used cold spinning technology in the process of actual production. The result of spinning form is influenced by the spindle speed. However, both the roughness of the part surface and the production efficiency can be improved by the appropriate speed.

The spindle speed is high means that the area in the deformation zone has increased in unit time. The results are that the circumferential flow of material is restrained effectively and the deformation conditions of work piece is improved. Therefore, the high dimensional accuracy and surface quality

of work piece can be ensured. However, the vibration of machine tool will be caused by over high speed. So the spindle speed set at 500 r/min seems rational. Generally there are three kinds of path curve for ordinary spinning of flat work pieces, which are oblique line, convex curve and concave curve respectively according to files[9]. The forming of blank is simulated by concave curve since it is the best common one among all the curves. The specific process parameter values are shown in table 1.

**Table 1.** Spinning Parameter Selection for Numerical Simulation of the Flywheel.

Parameter		Value
Blank	OD/mm	284
	ID/mm	40
	Thickness/mm	3
Parameter	Spindle Speed/ $r \cdot min^{-1}$	500
	Feed ratio of spinning roller/ $mm \cdot r^{-1}$	0.5 ,0.75,1.0
	Wall Thickness rReduction / $D_t$ (%)	50
	Spinning Temperature/ $^{\circ}C$	20
Path Curve for Spinning Roller	oblique line, convex curve and concave curve	concave curve

## Analysis of Simulation

### Feed ratio on the simulation analysis.



**Fig. 6.** Simulation Results of Three Different Feed Ratios

It is shown that the simulation results of three different feed ratios were processed by spinning of 0.5,0.75,1 in the Fig. 6. The feed ratio of 0.5 and feed ratio of 0.75 can meet the requirements of parts size, feed ratio of 0.5 appears uneven thickness slightly, feed ratio of 1 appeared incomplete forming after analysis.

### Strain field analysis.

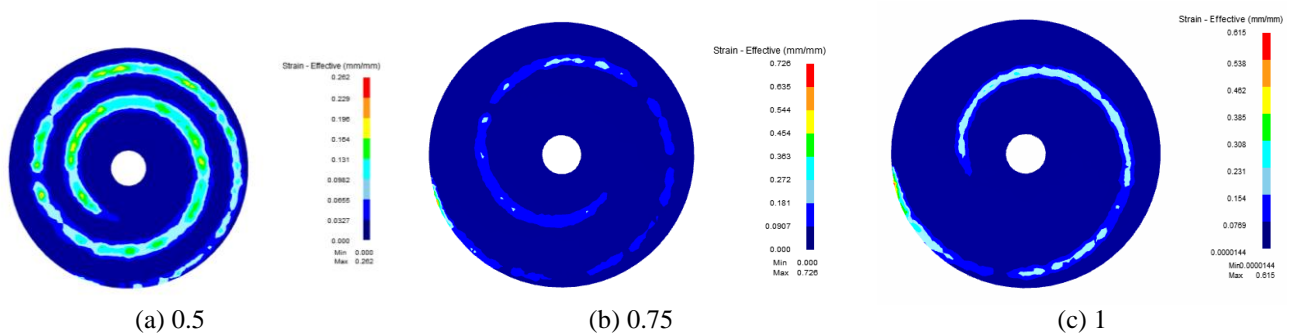


**Fig. 7** Strain Diagram of Three Different Feed Ratios

It is shown that strain diagram of three different feed ratios were processed by spinning of 0.5, 0.75, 1 in the Fig. 7. The strain value of distribution is below 0.2 under the feed ratio of 0.5 and 0.75, then the strain value of distribution is at 0.3 under the feed ratio of 1 from the above diagram.

### Stress field analysis.

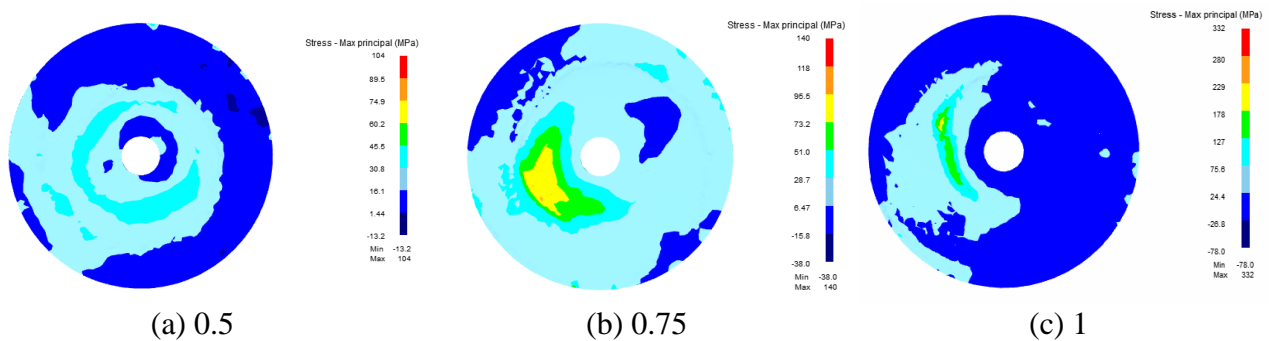


**Fig.8** Stress Diagram of Three Different Feed Ratios

It is shown that stress diagram of three different feed ratios were processed by spinning of 0.5, 0.75, 1 in the Fig. 8. The region of the maximum principal stress spread across the position of the blank slope into the plane. The maximum principal stress of feed ratio 0.5 is 105MPa, The maximum principal stress of feed ratio 0.75 is 140MPa and the maximum principal stress of feed ratio 1 is 332MPa.

## Spinning Press Analysis.

### Direction of X Axis.

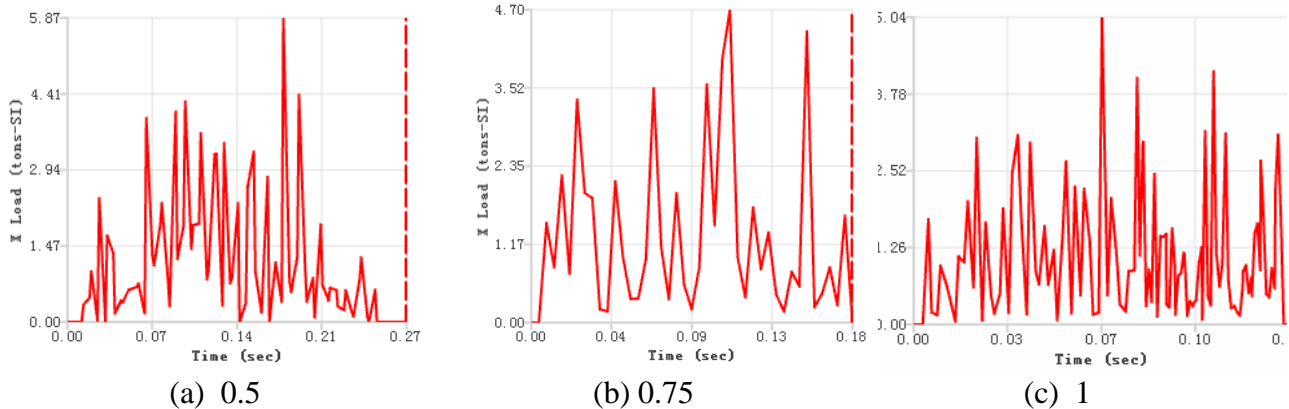


**Fig.9** Spinning Press of Direction X

It is shown that the spinning press curves of direction X are simulated at the feed ratio of 0.5, 0.75 and 1 in the figure 9. Where the maximum of the spinning press of direction X is 5.87 tons at the feed ratio of 0.5. When the feed ration is 1, the average spinning press is the minimum.

### Direction of Y Axis.

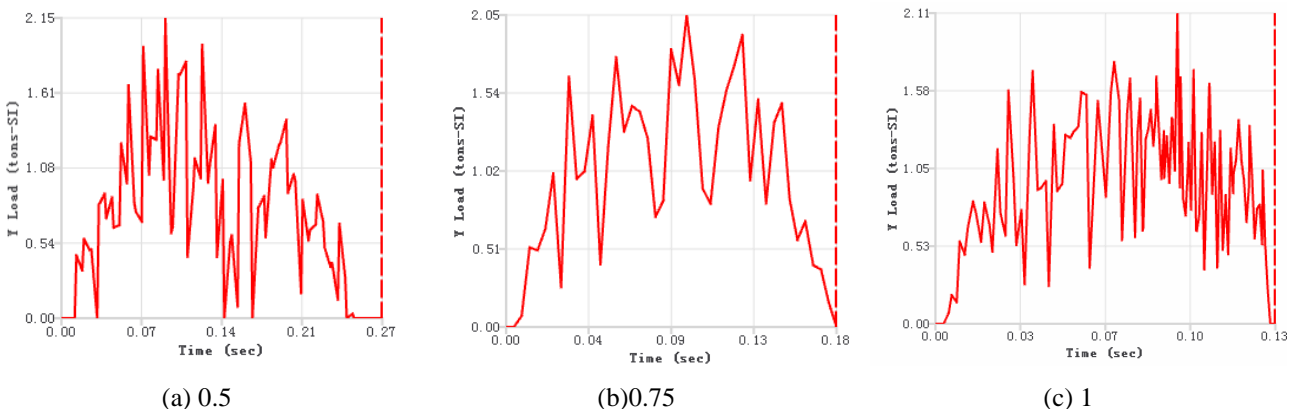


**Fig.10.** Spinning Press of Direction Y

It is shown that the spinning press curves of direction Y are simulated at the feed ratio of 0.5, 0.75 and 1 in the figure 10. Where the maximum of the spinning press of direction Y is 2.15 tons at the feed ratio of 0.5. When the feed ration is 1, the average spinning press is the minimum.

### Direction of Z Axis.

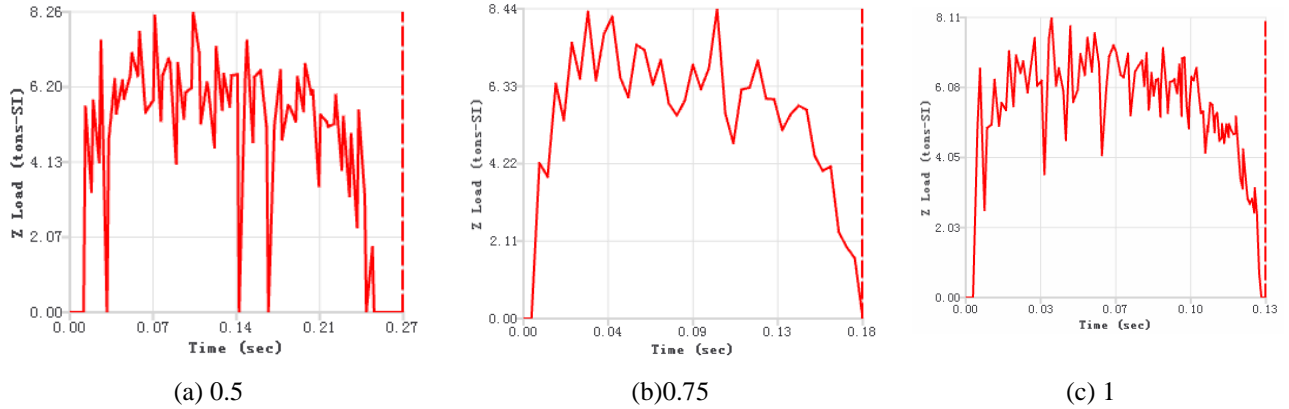


**Fig.11.** Spinning Press of Direction Z

It is shown that the spinning press curves of direction Z are simulated at the feed ratio of 0.5, 0.75 and 1 in the figure 11. Where the maximum of the spinning press of direction Z is 8.44 tons at the feed ratio of 0.75. When the feed ratio is 1, the average spinning press is the minimum.

## Results

- (1) The region of strain value spreads below 0.2 at the feed ratio of 0.5 and 0.75, while the region of strain value spreads about 0.3 at the feed ratio of 1 through the analysis of three feed ratio;
- (2) The maximum principal stress of feed ratio 0.5 is 105MPa, The maximum principal stress of feed ratio 0.75 is 140MPa and the maximum principal stress of feed ratio 1 is 332MPa;
- (3) The regions of maximum stress value for three feed ratios spread along the position of spinning roller. There is no difference in three each other about the maximum stress. They are 947MPa, 974MPa and 948MPa respectively;
- (4) The valve of spinning press at the feed of 1 is the lowest than the other two feed ratios after the analysis of three feed ratio;
- (5) There is no difference in the value of stress, strain and spinning press due to the small plastic deformation. The feed ratio of 0.75 meets the requirement at the size precision. Therefore it is suggested that the feed ratio of 0.75 is rational.

## Acknowledgement

Fund: Teachers in higher vocational colleges as senior engineers in jiangsu province in 2015(2015FG033).

## References

- [1] HU Xiao-jun, LI Xiao-ping. CAE Application Tutorial Plastic Forming by DEFORM-3D, Beijing: Beijing University Press(2011)
- [2] Japan Plastic Processing Society. Spinning Forming Technology [M], CHEN Jing-zhi, Translate. Beijing : Mechanical Industry Press(1986)
- [3] WANG Cheng-he, LIU Ke-zhang. Spinning Technology [M]. Beijing: China Machine Press(1986)
- [4] CHEN Shi-xian. Power Spinning Technology and Equipment[M], Beijing: National Defence Industry Press(1986)
- [5] XU Hong-lie. Power Spinning Technology [M]. Beijing: National Defence Industry Press(1984)
- [6] Kim S Y, Im Y T. Three-dimensional finite element analysis of non-isothermal shape rolling [J]. Journal of Materials Process Technology(2002)
- [7] YAN Zheng-feng. Design for Dual Mass Flywheel and Research in Manufacture Key Technology[D], Wuhan: Wuhan Technology University(2009)
- [8] CHEN Ru-xin, HU Zhong-mi. Elastoplastic Finite Element Method and Application in Metal Forming [M]. Chongqing: Chongqing University Press(1989)
- [9] Hayma M, Kudo H. Shinokura T. Study of the pass schedule in conventional simple spinning[J]. Bulletin of JSME( 1970)